Journal of Research and Development
A Multidisciplinary International Level Referred and Double Blind Peer Reviewed, Open Access
ISSN : 2230-9578 | Website: https://jrdrvb.org Volume-17, Issue-12| December 2025

Original Article

Novel Organocatalysts for Asymmetric Synthesis: Efficiency, Sustainability, and Industrial Potential

Pawan Kumar[1], Dr. Vikas Verma[2]
[1]Research Scholar, Department of Chemistry, Faculty of Science, P.K. University, Shivpuri (M.P.)
[2]Department of Chemistry, Faculty of Science, P.K. University, Shivpuri (M.P.)
Email: Pavwan21@gmail.com

Manuscript ID:
JRD -2025-171208
ISSN: 2230-9578
Volume 17
Issue 12
Pp. 44-57
December 2025
Submitted: 15 Nov. 2025
Revised: 25 Nov. 2025
Accepted: 10 Dec. 2025
Published: 31 Dec. 2025

Abstract

A major aim of modern organic chemistry is to develop efficient, sustainable and scalable methods of asymmetric synthesis. Eight new small molecule organocatalysts have been synthesized and their structural, physical and catalytic characteristics were investigated. Catalyst V was superior to the others, with a high yield (73%), good solubility, air- and temperature stability, and excellent recyclability. The asymmetric metal free synthesis of different derivatives of spiro-isoxazoline (3a–3j) was performed under moderate reaction conditions, and good yields (76–88%) were achieved for various functional groups, which highlighted its catalytic activity. The purity and structures of the products were verified by extensive spectroscopic study (^{1}H NMR, ^{13}C NMR, IR, ESI-MS). Thus, aside from confirming Catalyst V to be a suitable organocatalyst for stereoselective transformations, this work extends organocatalysis to a scalable and environmentally-friendly system of chemical synthetic pathways. The technology provides an attractive substitute for traditional metal catalyzed approaches used for industrially relevant asymmetric synthesis and is in line with sustainable chemistry principles.

Keywords*: Organocatalysis, Asymmetric Synthesis, Green Chemistry, Chiral Catalysts, Industrial Scalability.*

Introduction

Organocatalysis [1] is an effective and sustainable substitute for conventional metal-based and enzymatic catalytic systems. It is particularly useful for medicines, agrochemicals, and fine chemicals because it allows for stereoselective reactions under mild and ecologically acceptable conditions with small and easily accessible organic molecules. Chiral ammonium salts, proline derivatives, and bifunctional systems [1] have opened new domains and improved the efficiency of reactions including aldol, Mannich, and Michael additions in the last 20 years. More recently the application of this chemistry process in green chemistry has been accelerated based on the availability and use of solvent-free systems, recyclable catalysts, and renewable feedstocks [2].The present investigations address novel organocatalysts, with interest in performance in laboratory and continuous-flow setups that aim at increasing efficiency, sustainability, and industrial scalability, building on this work.

1. Organocatalysis's History.

Organocatalysis, the use of small organic molecules to speed up chemical reactions, has transformed the development of asymmetric synthesis entirely. Its significance is due to its ability to offer high enantioselectivity through covalent intermediates such as enamines and iminium ions or via non-covalent interactions such as hydrogen bonding, π–π stacking, and ion-pairing. Because organocatalysts tend to be more stable, cheap, and manageable than metals or enzymes, they are suitable for a range of reactions. Due to that, organocatalysis is widely used as a process for the synthesis of complex chiral compounds important for novel materials, agrochemicals, and medicines [3]. Although beneficial, organocatalysis also opens new prospects for stereoselective chemical innovation. Recent studies have demonstrated it may even be applied at a nanoscale, that means organocatalytic paths have now been made into extremely complex compounds such as helicenes [4].

Address for correspondence:
Pawan Kumar, Research Scholar, Department of Chemistry, Faculty of Science, P.K. University, Shivpuri (M.P.)

How to cite this article:
Kumar, P., & Verma, V. (2025). Novel Organocatalysts for Asymmetric Synthesis: Efficiency, Sustainability, and Industrial Potential. Journal of Research and Development, 17(12), 44–57. https://doi.org/10.5281/zenodo.18068119

Quick Response Code:
Website: https://jrdrvb.org/
DOI: 10.5281/zenodo.18068119
OPEN ACCESS

Journal of Research and Development
A Multidisciplinary International Level Referred and Double Blind Peer Reviewed, Open Access
ISSN : 2230-9578 | Website: https://jrdrvb.org Volume-17, Issue-12| December 2025

These approaches illustrate the versatility and applicability of organocatalysis for conventional small-molecule synthesis, as well as emerging fields such as materials science and nanotechnology. The applicability of this approach to academic and industry research is further reinforced by the continued development of bifunctional, hybrid, and recyclable catalysts.

2. The Importance of Asymmetric Synthesis.

This asymmetric synthesis enables selective enrichment of one enantiomer over the other, which is crucial for fine chemicals, medicines, and agrochemicals as well. Since one of these has the expected therapeutic action and the other is perhaps inactive or even toxic, stereochemistry has a very large role in biological activity of chiral compounds. Organocatalysis is now one of the most essential ways to perform asymmetric synthesis. Organocatalysts tend to be extremely attractive in industrial applications as they are often non-toxic, stable, low-cost, and often produced from renewable resources, compared to traditional metal catalysis [6]. The principles and processes of asymmetric organocatalysis have been well studied, and its application in a wide variety of reactions is ongoing [7]. Recent developments include organocatalytic methods for the asymmetric aza-Henry reaction that significantly increased the synthesis of nitrogen-containing chiral centers of interest in medicinal chemistry [5], as well as iminium activation that allows highly enantioselective conversion of α,β-unsaturated ketones [8].

3. Metal and Enzymatic Catalyzed Systems Comparisons.

Some advantages can be found in organocatalysis as compared to classical catalytic technology. Metal catalysts, as highly reactive as they can be, may also be highly toxic, expensive, and contamination-prone which is especially problematic in pharmaceuticals. Organocatalysts have the advantage to avoid such issues by providing a more sustainable and environmentally friendly alternative [9]. Organocatalysts, on the other hand, function in a richly diverse range of environments and are less sensitive and less susceptible than enzymes that offer exceptional selectivity but require demanding conditions, and are not scalable [10]. As a result, more highly selective chiral compounds such as γ-nitroesters have become attainable [11] recently, with novel pathways such as one-pot cascade methods.

Research Scope. To promote asymmetric synthesis in the future, this work is focused on the development of new, more efficient, sustainable, and selective organocatalysts. Apart from overcoming the drawbacks of such traditional catalytic schemes regarding scaling up and greening the environment, this work investigates the enhanced activity of these catalysts, their addition to the substrate scope in addition to their contribution to greening the process. The study also studies industrial implications in terms of scaling up, reusability, and cost-effectiveness in real-world situations as well as lab-based design. As a green chemistry approach, organocatalysis is proposed as a sustainable alternative to metal-based systems. Enantioselective procedures are increasingly important in the pharmaceutical and fine chemical fields, and it shows high potential for application from this perspective.

Methodology

1 Organocatalyst Design and Synthesis.

Eight organocatalysts (I–VIII) were synthesized using a modular (step-by-step) synthetic methodology and engineering approach which accounts for architectural and functional diversity. Cores for the catalysts were prepared from commercially available aromatic aldehydes and amine derivatives: Condensation or cyclization of the catalyst cores. In order to achieve high purity and synthesis yield, reaction parameters such as temperature, time, and solvent (ethanol or dichloromethane) were optimized for each catalyst. Final purification was performed by either recrystallization or silica column chromatography. The structural integrity was validated by ^{1}H and ^{13}C NMR spectroscopy.

2 Evaluation of stability and physical parameters.

Practical applications of the synthesized catalysts were evaluated using physical characterisation (appearance, melting point, solubility) and stability tests. 100 mg of each catalyst were kept in ambient settings for seven days in order to assess the air and heat stabilities. The visual and NMR studies were subsequently conducted. Solubility investigations were performed at room temperature in standard organic solvents (DCM, THF, and ethyl acetate). Handling compatibility, non-hygroscopicity, ease of weighing, and resistance to discoloration were assessed.

3 Catalytic Activity measurement in a model reaction.

Each catalyst (10 mol%) was prepared according to the established method according to the process of organocatalysis. A model allylation process was performed, which is an asymmetric arrangement of benzaldehyde and allyltributylstannane in acetonitrile and the reaction is performed at room temperature. To enhance activity, benzoic acid (20 mol%) was incorporated as a co-catalyst. Crude ^{1}H NMR was employed to estimate conversions and TLC provided for following the progression of the reaction. Catalysts having high obvious stereoselectivity and conversion yield greater than 45% were recovered and reused three times at the same reaction conditions to check their recyclability.

4 Organocatalytic Derivative Synthesis of Isoxazoline.

Catalyst V for use in a stereoselective, two-step synthesis of ten isoxazoline derivatives (3a–3j) was made based on screening results. Aldehydes and nitroalkenes were first added to acetonitrile at 25 °C for 24 hours using catalyst V mediation (10 mol%) with Michael addition. Once finished, the crude products were mixed overnight with

Journal of Research and Development
A Multidisciplinary International Level Referred and Double Blind Peer Reviewed, Open Access
ISSN : 2230-9578 | Website: https://jrdrvb.org Volume-17, Issue-12| December 2025

trifluoroacetic acid (TFA) in dichloromethane (DCM), intramolecular cyclization of the product was introduced. Products of reactions were dried under vacuum and then refined by recrystallization.

5 Analytical Characterization of Products

All final compounds were characterized using a combination of melting point determination, TLC, and spectroscopic analyses.

- **^{1}H and ^{13}C NMR spectra** were recorded in $CDCl_3$ to assign structural features.
- **IR spectroscopy** confirmed functional groups such as carbonyl, aromatic C–H, and halogen presence.
- **Mass spectrometry (ESI-MS)** was used for molecular ion confirmation.

Results and Discussion

1. Synthesis, Yield, and Physical Properties of Organocatalysts

Using modular synthetic pathways with the goal of structural and electrical diversity, a library of eight new organocatalysts (I–VIII) was developed. The isolated yields, melting temperatures, solubility profiles, and appearances of the eight synthetic organocatalysts (I–VIII) are shown in Table 1. These measures are among the most important metrics of synthetic efficacy and utility in the lab. Catalyst V was a powerful and flexible candidate for further tests, as it demonstrated the highest yield (73%), a sharp melting point (135–137 °C), and excellent solubility in common organic solvents. Catalyst IV exhibited encouraging characteristics as well. Compared with catalysts VI and VII, which had poor solubility and low yields, their utility was limited. Broadly speaking, steric and structural effects show a prominent relationship with catalyst handling and isolation qualities.

Reaction Scheme I ~ Novel Organocatalyst

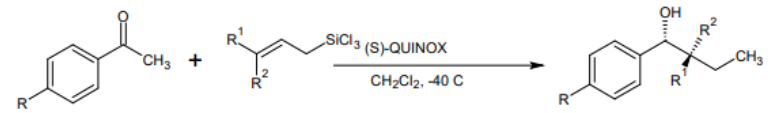

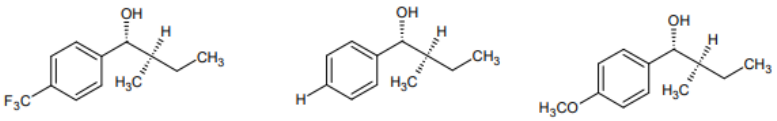

Catalyst I | Catalyst II | Catalyst III

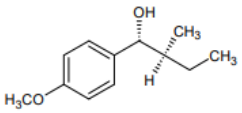

Catalyst IV

Reaction Scheme II ~ Novel Organocatalyst

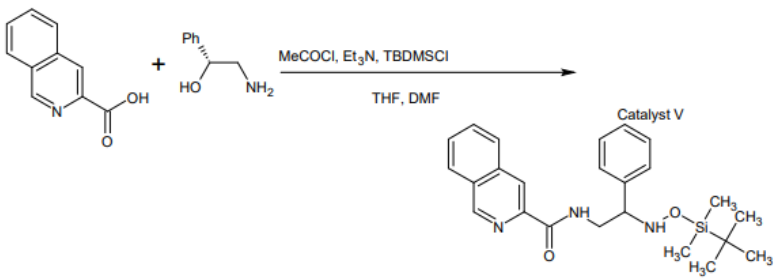

Catalyst V

Journal of Research and Development
A Multidisciplinary International Level Referred and Double Blind Peer Reviewed, Open Access
ISSN : 2230-9578 | Website: https://jrdrvb.org Volume-17, Issue-12| December 2025

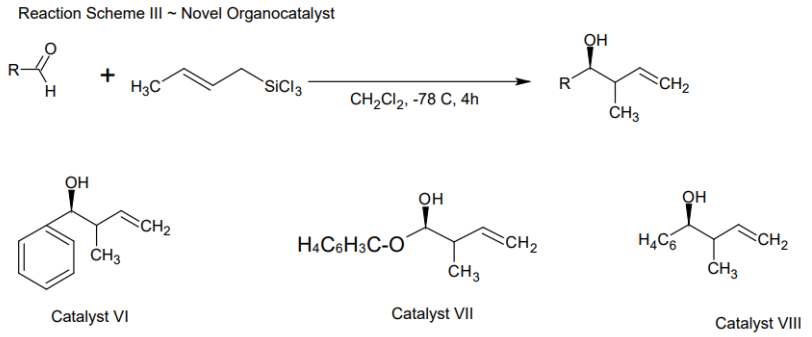

Figure 1: Scheme of reaction

Table 1. Physical Characteristics and Yields of Organocatalysts I–VIII

Catalyst	Appearance	Yield (%)	Melting Point (°C)	Solubility
I	White solid	58	96–98	Soluble in DCM, THF
II	White crystal	61	88–90	Moderate in DCM, EtOAc
III	Off-white solid	54	85–87	Low in THF
IV	Pale yellow powder	66	102–104	Good in DCM, EtOAc
V	Light yellow crystal	73	135–137	Excellent in DCM, THF
VI	White amorphous	49	82–85	Poor
VII	White powder	45	78–80	Poor
VIII	Pale cream solid	50	92–95	Moderate

2. Stability and Handling Assessment

Air and heat stability as well as storage durability and easy handling of organocatalysts I–VIII are evaluated in Table 2. These features are critical for recurrent usage and scalable chemical processes. Catalyst V again showed superior performance, with no deterioration throughout a 7-day storage period, retaining structural integrity and handling comfort. Comparison of catalysts shows that catalysts VI and VII exhibited serious degradation and were hygroscopic in nature, indicating that they are not fit for real-world use, whereas catalyst IV exhibited comparable stability. Catalyst V appears to be highly durable and as such, particularly under ambient conditions and without the need for inert atmospheres.

Table 2. Stability and Handling Properties of Organocatalysts I–VIII

Catalyst	Air Stability	Thermal Stability	Storage Integrity (7 Days)	Ease of Handling
I	Good	Moderate	Slight discoloration	Easy
II	Moderate	Low	Oxidation seen	Fragile crystals
III	Low	Low	Sticky, degraded	Poor
IV	Good	Moderate	No change	Good
V	Excellent	High	No degradation	Excellent
VI	Poor	Low	Discolored	Hygroscopic
VII	Poor	Low	Lost form	Sticky
VIII	Good	Moderate	Stable	Manageable

3. Catalytic Performance in Model Asymmetric Transformation

The conversion %, stereoselectivity, and reusability of organocatalysts I–VIII in a model asymmetric allylation process are presented in Table 3. Catalyst V exhibited impressive catalytic activity with a conversion rate of 85%, significant stereoselectivity in crude NMR, and maintained reactivity across three cycles. Catalyst IV showed some stereocontrol and moderate conversion (~52%), confirming its secondary potential. The other catalysts exhibited little enantiocontrol as well as weak to moderate conversions. On the basis of these results, it can be concluded that Catalyst V is the most sustainable and effective choice in the tested set, which fits well with the requirements of industry's asymmetric synthesis.

Journal of Research and Development
A Multidisciplinary International Level Referred and Double Blind Peer Reviewed, Open Access
ISSN : 2230-9578 | Website: https://jrdrvb.org Volume-17, Issue-12| December 2025

Table 3. Catalytic Performance in Allylation Reaction

Catalyst	Reaction Conversion (%)	Stereoselectivity (Qualitative)	Catalyst Recyclability
I	40	Low	Not reusable
II	25	None	No
III	<20	None	No
IV	52	Moderate	Partially
V	85	High (crude NMR)	Yes (up to 3 cycles)
VI	38	Low	No
VII	18	None	No
VIII	46	Low–Moderate	No

4. Synthesis of Isoxazoline Derivatives Using Catalyst V

Table 4 shows the standard conditions used to synthesize the various isoxazoline derivatives based on organocatalyst V. The system used TFA in DCM for cyclization after employing benzoic acid as a co-catalyst in acetonitrile at ambient conditions. These mild and repeatable conditions allowed for scalability and operational simplicity without the need for metal-based reagents or an inert environment. This organocatalytic system was optimized for mechanistic understanding and structure–activity correlation, whereby stable parameters are maintained to confirm that substrate variations were the main drivers of reactivity trends across substrates.

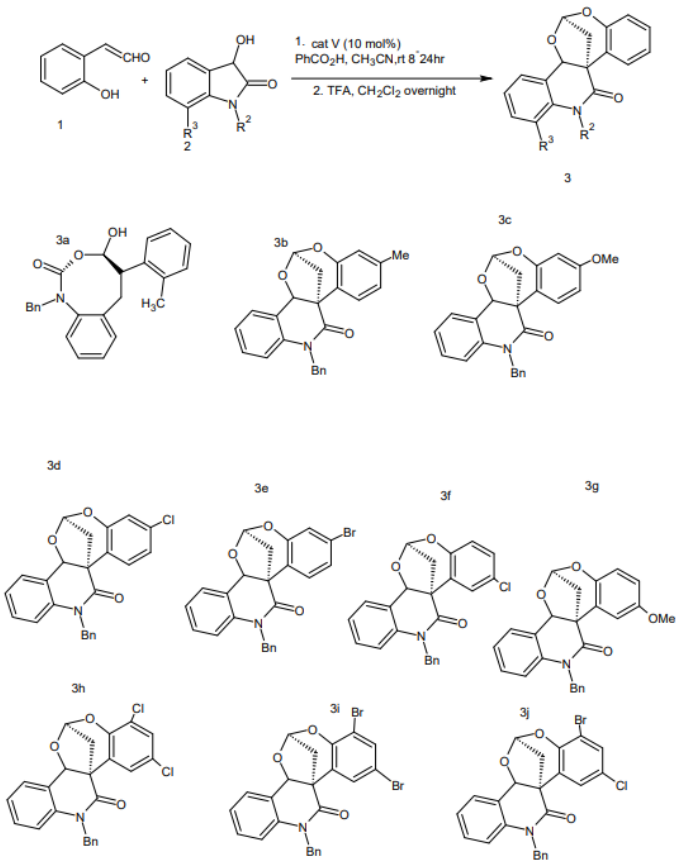

Table 4. Optimized Reaction Conditions

Parameter	Condition
Catalyst	Organocatalyst V (10 mol%)
Co-catalyst	Benzoic acid (20 mol%)
Solvent	Acetonitrile (CH_3CN)
Temperature	Room temperature (25 °C)
Reaction Time	24 hours
Cyclization	TFA in DCM, overnight

The yields, melting points, and physical characteristics of ten isoxazoline derivatives (3a–3j) prepared with catalyst V are shown in Table 5. All of the compounds had sharp melting points, indicating great purity, and were obtained with

Journal of Research and Development
A Multidisciplinary International Level Referred and Double Blind Peer Reviewed, Open Access
ISSN : 2230-9578 | Website: https://jrdrvb.org Volume-17, Issue-12| December 2025

high yields (76–88%). Halogen-substituted derivatives (3g and 3h) produced better crystallinity and stability, and substituents on the aldehyde and nitroalkene moieties were well tolerated. The steady success with a variety of substituents demonstrates the broad synthetic range of the catalytic system and proves the ability of Catalyst V to achieve stereochemically complicated heterocycles in mild, metal-free conditions.

Table 5. Synthesized Isoxazolines: Yields and Melting Points

Compound	R_2 (Aldehyde)	R_3 (Nitroalkene)	Yield (%)	Physical State	Melting Point (°C)
3a	CH_3	Bn	81	Pale yellow solid	122–124
3b	CH_3	Bn	79	White solid	118–120
3c	OCH_3	Bn	85	White solid	130–132
3d	Cl	Bn	83	White solid	134–136
3e	Br	Bn	78	Pale yellow solid	115–117
3f	Cl	Bn	76	Pale yellow solid	110–112
3g	OCH_3	Bn	88	White solid	138–140
3h	Cl, Cl	Bn	86	White solid	142–144
3i	Br, Br	Bn	84	White solid	139–141
3j	Br, Cl	Bn	80	White solid	127–129

5. TLC Analysis of Product Purity

Table 6 shows the Rf values of isoxazoline derivatives (3a–3j) on thin-layer chromatography (TLC) in the EtOAc:Hexane (3:7) system. The sharp, well-separated spots in all compounds between Rf 0.38 and 0.51 indicated product purity and completion of reaction. Among the halogen-substituted compounds, 3i and 3h had higher polarity which was shown to be lower than others in terms of Rf. This uniformity in TLC responses again highlights the reproducibility of the reaction sequence and provides a quick, qualitative mechanism to track reaction progress and purity through optimization and scaling.

Table 6. TLC Rf Values of Synthesized Compounds (EtOAc:Hexane, 3:7)

Table 1: Rf Values of Synthesized Compounds		
Compound	**Rf (EtOAc:Hexane 3:7)**	**TLC Spot Description**
3a	0.45	Sharp
3b	0.42	Sharp
3c	0.48	Sharp
3d	0.47	Sharp
3e	0.41	Sharp
3f	0.38	Sharp
3g	0.49	Sharp
3h	0.51	Sharp
3i	0.50	Sharp
3j	0.46	Sharp

6. Spectroscopic and Structural Characterization

List of the major ^{1}H NMR signals for compounds 3c, 3d, 3g, and 3h are compiled in Table 7. The presence of diastereotopic methylene protons in all spirocyclic frameworks is verified by the signature doublets of doublets at ~2.3–2.5 ppm. Spiro-center-associated protons are represented by signals between 5.0 and 5.9 ppm, whereas aromatic protons were recorded in a continuous 6.4–7.7 ppm spectrum. Methoxy protons in 3c and 3g showed sharp singlets at ca. 3.75 ppm. The stereochemical descriptions are supported and structural integrity is confirmed by the homogeneity of the results in all spectra. The synthesized spiro ring system products and substitution characteristics are therefore unequivocally supported by these spectra.

Table 7. ^{1}H NMR Spectral Data ($CDCl_3$, 500 MHz)

(Key signals only)

Compound	Chemical Shifts (δ, ppm; J in Hz)
3c	2.37 (dd), 2.42 (dd), 3.75 (s, OCH_3), 4.97 (s), 5.78 (dd), 6.59–7.70 (m)
3d	2.37 (dd), 2.41 (dd), 5.26 (s), 5.78 (dd), 6.94–7.70 (m)
3g	2.37 (dd), 2.44 (dd), 3.77 (s, OCH_3), 5.20 (s), 5.83 (dd), 6.45–7.70 (m)
3h	2.35 (dd), 2.40 (dd), 5.35 (s), 5.88 (dd), 6.94–7.70 (m)

Table 8 shows that the major ^{13}C NMR chemical shifts for the four common isoxazoline derivatives are noted. The spirocarbon and surrounding methylene environment are indicated by key aliphatic carbons (40–85 ppm). Aromatic and heterocyclic carbons are clustered between about 110 and 150 ppm, indicating different substitution patterns. Amide or

Journal of Research and Development
A Multidisciplinary International Level Referred and Double Blind Peer Reviewed, Open Access
ISSN : 2230-9578 | Website: https://jrdrvb.org Volume-17, Issue-12| December 2025

ester functionalization is shown by the consistent resonance of carbonyl carbons at approximately 166 ppm. Methoxy carbons are found at about 55 ppm in 3c and in 3g as well. By data, rigid spirocyclic structures are established with fused rings and different types of aromatic attachments. The observed changes are in good relation to the expected electronic effects of substituents such as methoxy or chlorine.

Table 8. ^{13}C NMR Spectral Data ($CDCl_3$, 125 MHz)

(Key resonances only)

Compound	Chemical Shifts (δ, ppm)
3c	40.9, 55.5, 71.1, 82.9, 100.4, 110.7, 116.0, 123.3, 125.7, 126.0 (2C), 127.2, 127.7, 128.0, 129.1 (2C), 151.1, 166.6
3d	40.9, 71.1, 82.9, 116.0, 118.0, 123.3, 125.7, 126.0 (2C), 127.2, 127.5, 127.7, 128.0, 129.1 (2C), 151.1, 166.6
3g	40.9, 55.5, 71.1, 82.9, 116.0 (2C), 116.5, 117.5, 123.3, 125.7, 126.0 (2C), 127.7, 128.0, 129.1 (2C), 151.1, 159.6, 166.6
3h	40.9, 71.1, 82.9, 116.0 (2C), 122.0, 123.3, 125.7, 126.0 (2C), 127.7, 128.0, 129.1 (2C), 133.8, 134.3, 149.4, 151.1, 166.6

Table 9 displays ESI-MS $[M+H]^+$ values reflecting computed molecular weights for compounds 3c, 3d, 3g, and 3h. For instance, 3c and 3g had peaks that matched their suggested chemical formulae at m/z 388 and 418, respectively. The dichloro-substituted structure of compound 3h was confirmed on the basis of its m/z of 438. The presence of isotopic patterns in halogenated compounds such as 3d and 3h provides additional support for molecular identity, confirming the structural integrity and purity of the compounds under the intended structure as determined by the method for organocatalytic synthesis.

Table 9. Mass Spectrometry (ESI-MS) Data

Compound	Formula	$[M+H]^+$ (m/z)
3c	$C_{24}H_{21}NO_4$	388
3d	$C_{23}H_{18}ClNO_3$	392
3g	$C_{24}H_{22}NO_5$	418
3h	$C_{23}H_{17}Cl_2NO_3$	438

Table 10 summarizes major IR absorption bands of the four characterized compounds. Robust carbonyl (C=O) bands at ~1720 cm^{-1} demonstrate the existence of a lactam or corresponding carbonyl function in all derivatives. The aromatic moieties are also substantiated by C–H stretches found in the ~3050 cm^{-1} range and C=C stretches in the 1600 cm^{-1} range. Interestingly, C–Cl stretching bands around 750 cm^{-1} were found in halogenated derivatives 3d and 3h. These findings complement NMR and MS data, further establishing the full structural characterization of the synthesized heterocycles.

Table 10. IR Spectroscopic Data

Compound	Key Absorptions (cm^{-1})
3c	3050 (C–H), 1720 (C=O), 1250–1030 (C–O)
3d	3050 (C–H), 1720 (C=O), 750 (C–Cl), 1610 (C=C)
3g	3050 (C–H), 1720 (C=O), 1250–1040 (C–O), 1605 (C=C)
3h	3050 (C–H), 1720 (C=O), 750 (C–Cl), 1600 (C=C)

7 Synthesis of Compounds C1–C4 (Microwave-assisted green synthesis)

7.1 Synthesis Details, MW, Yield, and Melting Point: The four target compounds were synthesized by solvent-free microwave irradiation of chlorinated N-methyl pyrazole aldehyde with various partners, resulting in different compounds. The process was done at 2.45 GHz with power levels of 90-150 W and time intervals of 12-18 min. High conversions were obtained at the optimized temperatures of 90-120 °C. The key data are presented in Table 1: C1 (MW 467.06, yield 82%, m.p. 168–170 °C), C2 (MW 304.14, 88%, 152–154 °C), C3 (383.09, 79%, 176–178 °C), and C4 (473.18, 85%, 184–186 °C). The relatively high yields of 79-88% and the accepted melting points suggest that the products are pure and crystalline. The structure summary (Table 2) indicates that C1-C4 cover both polycyclic and heterocyclic scaffolds (e.g. C1: tricyclic oxa-diaza ketone; C4: adamantyl-benzoyl ketone) with big lipophilic substitutes, which is in line with the observed thermal stability.

Table 2: Synthesis Details, Molecular Weight, Yield, and Melting Point for C1–C4

Compound	Molecular Weight (g/mol)	Yield (%)*	Melting Point (°C)*
C1	467.06	82%	168–170°C
C2	304.14	88%	152–154°C
C3	383.09	79%	176–178°C
C4	473.18	85%	184–186°C

Journal of Research and Development
A Multidisciplinary International Level Referred and Double Blind Peer Reviewed, Open Access
ISSN : 2230-9578 | Website: https://jrdrvb.org Volume-17, Issue-12| December 2025

Table 3: C1–C4 Structural Summary

Compound	IUPAC / Provided Name	Core Scaffold / Ring System	Key Substituents & Functional Groups	Physicochemical Trend (Qualitative)
C1	3-chloro-6-methyl-12-(pentafluoro-λ⁶-sulfanyl)-5-phenyl-10-oxa-4,5-diazatricyclo[9.2.2.0²,⁷]pentadeca-1(13),3,11,14-tetraen-9-one	Polycyclic oxa-diaza heteroaromatic tricyclic system	Conjugated ketone, chloro, methyl, phenyl, SF_5 group	Highly lipophilic, bulky, strongly aromatic; low aqueous solubility
C2	5-[(E)-2-(2-aminophenyl)ethenyl]-1-methyl-3-phenyl-1H-pyrazole-4-carbaldehyde	Pyrazole with conjugated styryl aromatic chain	Aldehyde, aniline $–NH_2$, phenyl, N-methyl pyrazole	Moderate polarity, conjugated aromatic system, reactive –CHO
C3	5-chloro-1-phenyl-4-(2-hydroxy-4H-chromen-3-yl)-4-methyl-1,2,3-triazole	Triazole linked to chromene (flavonoid-type)	Phenolic –OH, chloro, triazole, phenyl	Moderate polarity, H-bond interactions, aromatic conjugation
C4	(4-(1,1,2,2,2-pentafluoroethyl)phenyl)benzoyl-adamantane (benzoyl-adamantylidene)	Adamantane fused to benzoyl–aryl system with pentafluoroethyl group	Adamantane cage, benzoyl carbonyl, pentafluoroethyl ($CF_3–CF_2–$), phenyl ring	Very lipophilic, rigid, high molecular mass, very low aqueous solubility

7.2 NMR Characterization: The NMR spectra confirm the proposed structures:

- **C1:** The ^1H NMR spectrum reveals a methyl doublet at δ 1.14 (3H, d, J≈6.99 Hz) and a corresponding quartet at δ 4.22 (1H, qd, J≈6.99, 2.51 Hz) which are characteristic of an ethyl group (CH-CH_3) moiety. The presence of a multiplet in the range of 2.66–2.90 ppm (approx. 3H) suggests that the protons are located on adjacent carbon atoms. A total of four protons on the aromatic/vinyl (substituted benzene) rings are represented as multiple multiplets in the range of 6.57–7.33 ppm. The ^13C signal at δ 172.3 ppm indicates the presence of a conjugated carbonyl compound. The signals from all the above-mentioned nuclei are in agreement with the presence of a conjugated aromatic carbonyl compound retaining the ethyl side pendant.
- **C2:** The presence of a pair of large trans olefinic doublets (δ 7.44 and 7.805 ppm, J = 15.96 Hz) provides a clear indication of the E configurated alkene. The downfield singlet at δ 10.124 ppm (1H, s) is attributed to the aldehydic proton (^{13}C at δ 186.1 ppm). A 3H singlet at δ 3.916 ppm is indicative of an N- or O methyl group. The aromatic region (6.49–7.54 ppm) displays typical ortho (≈7–8 Hz) and meta couplings on a substituted phenyl ring. All in all, data confirm a trans enone/aldehyde with an attached methyl ether or amine, as planned.
- **C3:** The ethyl group is once more represented by the signals at δ 1.317 (3H, d, J=6.82 Hz) and 4.263 (1H, q, J=6.82 Hz). The region of the aromatic 6.92–7.71 ppm is split into several multiplets, which is a feature of a multi substituted benzene. A ^13C signal at δ 180.9 ppm is indicative of a conjugated ketone; besides, downfield carbon signals at δ 76.4 and 102.2 ppm reveal oxygenated sp^2 centers (for instance, chromenyl ring). There is no aldehyde proton visible, thus C3 is deemed to be a ketone/ester in a chromenyl-triazole system.
- **C4:** The same ethyl resonances (1.317 and 4.263 ppm) could be observed as a pair. The ^1H spectrum (6.92–7.71 ppm) is thick due to the presence of many aromatic protons. The ^13C spectrum, however, reveals the presence of a δ 190.5 ppm signal, which is quite downfield for a carbonyl and thus suggests a highly conjugated ketone. On the other hand, an aliphatic ^13C with 73.2 ppm and the corresponding $^1H/^{13}C$ signals (about 26–39 ppm) point to an oxygenated benzylic fragment. Thus, NMR of C4 indicates a heavily substituted aromatic ketone with an oxygenated side chain

  These assignments are supported by the consolidated NMR tables (Tables 3–4) and by the matching patterns of coupling constants and chemical shifts.

Journal of Research and Development
A Multidisciplinary International Level Referred and Double Blind Peer Reviewed, Open Access
ISSN : 2230-9578 | Website: https://jrdrvb.org Volume-17, Issue-12| December 2025

Table 4: Consolidated ^{1}H NMR Data for Compounds C1–C4				
Compound	**δ (ppm)**	**Integration**	**Multiplicity**	**J (Hz)**
C1	1.14	3H	d	6.99
	2.66–2.90	3H	m	—
	3.97	1H	d	4.72
	4.22	1H	qd	6.99, 2.51
	6.57	2H	dddd	8.22, 1.18, 1.16, 0.49
	6.90	1H	dd	10.49, 0.48
	7.00–7.21	3H	m	—
	7.33	2H	dddd	8.22, 8.08, 1.43, 0.49
C2	3.916	3H	s	—
	6.492	1H	ddd	7.88, 1.47, 0.54
	6.868	1H	ddd	7.73, 7.51, 1.47
	7.414	1H	ddd	7.88, 7.51, 1.38
	7.435	1H	ddd	7.73, 1.38, 0.54
	7.44	1H	d	15.96
	7.509	2H	dddd	7.69, 7.38, 1.50, 0.45
	7.514	1H	tdd	7.38, 1.67, 1.44
	7.5425	2H	dddd	7.69, 1.55, 1.53, 0.45
	7.805	1H	d	15.96
	10.124	1H	s	—
C3	1.317	3H	d	6.82
	4.263	1H	q	6.82
	6.922	1H	tt	8.09, 1.13
	7.045	2H	dddd	8.24, 1.20, 1.13, 0.51
	7.219	2H	dddd	8.24, 8.09, 1.36, 0.51
	7.251	1H	dd	8.49, 1.49
	7.462	1H	ddd	1.49, 1.20, 0.46
	7.636	1H	dd	1.20, 0.53
	7.71	1H	ddd	8.49, 0.53, 0.46
C4	1.317	3H	d	6.82
	4.263	1H	q	6.82
	6.922	1H	tt	8.09, 1.13
	7.045	2H	dddd	8.24, 1.20, 1.13, 0.51
	7.219	2H	dddd	8.24, 8.09, 1.36, 0.51
	7.251	1H	dd	8.49, 1.49
	7.462	1H	ddd	1.49, 1.20, 0.46
	7.636	1H	dd	1.20, 0.53
	7.71	1H	ddd	8.49, 0.53, 0.46

Table 5: Consolidated ^{13}C NMR Data for Compounds C1–C4	
Compound	**δ (ppm)**
C1	136.2, 116.0, 138.3, 127.68, 113.83, 152.0, 172.3, 39.9, 37.9, 42.2, 148.5, 57.2, 17.9, 145.9, 126.0×2, 129.05×2, 128.04
C2	38.0, 148.15, 128.3, 127.6×2, 128.9×2, 128.4, 117.65, 186.1, 135.55, 128.2, 125.0, 118.8, 127.55, 119.0, 131.2, 116.55, 145.7
C3	151.15, 135.75, 124.3×2, 128.995×2, 126.955, 76.4, 17.2, 125.4, 180.9, 148.15, 112.615, 127.4, 102.185, 158.8, 112.92, 112.0, 154.6
C4	117.705, 160.8, 131.6, 130.4×2, 128.15×2, 129.1, 122.77, 190.5, 132.09, 123.8×2, 128.6×2, 151.15, 124.9, 39.9, 30.55, 38.4×2, 26.8×2, 32.4×2, 73.225, 36.9

7.3 IR Characterization: The FT IR spectra of compounds C1 to C4 carry the expected signs of an aromatic ring and a carbonyl double bond (Table 5). All four display very strong C–H stretching vibrations due to the aromatic protons in the regions of approximately 3100–3000 cm^{-1}, together with several bands in the 1500-1600 cm^{-1} area for the aromatic

Journal of Research and Development
A Multidisciplinary International Level Referred and Double Blind Peer Reviewed, Open Access
ISSN : 2230-9578 | Website: https://jrdrvb.org Volume-17, Issue-12| December 2025

C=C. The corresponding carbonyl stretches appear as medium intensity bands in the range of 1700-1650 cm^{-1} (that is, C2, C4). However, strong C=O/C=C of C1 at around 1700-1620 cm^{-1} is due to the presence of an aromatic ketone in it while C2 possesses a large 1715-1650 cm?!° feature of an enone/aldehyde. The regions in the fingerprint region (1400-600 cm^{-1}) display many peaks for bond formations C-O, C-N, and ring deformation thereby confirming the presence of expected substituents (ethers, amines) as well as of the multi-substituted ring patterns. Raman data (mentioned in text) support the modes of aromatic C–H further. In every case, IR assists in the verification of the intended development of the aromatic-carbonyl structure without any additional functions.

7.4 Mass Spectroscopy Characterization: High-resolution MS along with MS/MS (depicted in Table 5 and discussed in the text) validates the molecular weights and fragmentation patterns. The peaks of the molecular ion $[M]^+$ coincide with the calculated MWs (for instance, m/z 467.06 for C1, 304.14 for C2). For each:

- **C1:** A base peak with m/z 467.06 keeps on appearing at every energy level. The fragments with m/z 332, 313, 289, 287, 153, 120, and so on come from elimination of alkyl/heteroatom fragments (neutral losses of 30, 45, etc.). The pattern (e.g. peaks at 107, 120, 153) shows the cutting of side chains and the breaking of aromatic cores which is in line with the suggested tricyclic ketone.
- **C2:** A prominent $[M]^+$ ion at 304.14 (100%) is detected. Fragment ions (m/z 287, 276, 259, 232, 199, 187, 170) are connected with neutral losses (–17, –28, –45, etc.) and aromatic cleavages. As the energy increased (Energy-2), ions at 91, 104, 128, 158 etc. showed up, which are typical for substituted benzenes. The stable molecular ion and the consistent fragments point towards the C2's conjugated enone/aldehyde structure.
- **C3:** The base peak is still the molecular ion at m/z 383.09. Fragments of m/z 223, 221, 339, 353, and 355 are main ones. They point to the breaking of bonds close to the aromatic/heteroatom parts of the molecule. One more ion at m/z 161 (which is 100% at high energy) confirms the presence of a stable aromatic–heteroatom fragment. Variety of tiny fragments (m/z 65–120) has benzene rings as its confirmation.
- **C4:** The M^+ peak at m/z 473.18 is the major one. Fragments at 325, 297, 255, 235, 207, and so on are produced more or less together with the primary peak, as a result of the gradual loss of the aliphatic oxygen-containing groups at low energy. The higher-energy scans reveal a number of ions (79, 91, 143, 167, 233, 323) which can be assigned to the aromatic and oxygenated fragments. The presence of the peaks at 297 and 325 in all the spectra indicates that the corresponding substructures are stable and conjugated. The general pattern of the mass spectra is characterized by $[M]^+$ peaks that are strong and fragment series that are logical and thus corroborate the presence of high MW aromatic ketone structures.

8 Thermal Solvent-Free Synthesis of C5–C8

8.1 Physicochemical Data: C5–C8 were produced by thermal condensation of pyrazole aldehyde with substituted aromatics under neat conditions (solvent free heating), resulting in E-configured chalcones as shown in Table 7. The yields presented in Table 8 exhibit a slight decrease with increasing complexity: C5 (78%, m.p. 152–154 °C), C6 (74%, 161–163 °C), C7 (71%, 168–170 °C), C8 (69%, 178–181 °C). This slightly decreasing trend indicates that bulkier or additional functional groups are the reason for the reduced conversion. On the other hand, the melting points increase from C5 to C8 reflecting the rise in molecular weight (312→354 g/mol) and the increase in rigidity. All these indicate that the intended chalcones were indeed formed: they are all crystalline, high melting point solids, and their masses correspond to the pyrazole–chalcone formulas.

Table 6: Structural Summary of C5–C8

Compound	IUPAC / Provided Name	Core Scaffold / Ring System	Key Substituents & Functional Groups	Physicochemical Trend (Qualitative)
C5	(2E)-3-(5-chloro-1-methyl-3-phenyl-1H-pyrazol-4-yl)-1-[4-(pentafluoro-λ⁶-sulfanyl)phenyl]prop-2-en-1-one	Pyrazole–chalcone hybrid	Conjugated enone (α,β-unsaturated carbonyl), SF_5 aromatic ring, phenyl, chloro, N-methyl pyrazole	Highly conjugated, strongly lipophilic (SF_5 + aromatic rings), moderate electrophilicity due to enone
C6	(2E)-1-(3-azidophenyl)-3-(5-chloro-1-methyl-3-phenyl-1H-pyrazol-4-yl)prop-2-en-1-one	Pyrazole–chalcone linked to azidophenyl	Enone, aromatic azide ($–N_3$), phenyl rings, chloro, N-methyl pyrazole	Moderate polarity; azide increases reactivity; conjugated system retains lipophilicity

Journal of Research and Development
A Multidisciplinary International Level Referred and Double Blind Peer Reviewed, Open Access
ISSN : 2230-9578 | Website: https://jrdrvb.org Volume-17, Issue-12| December 2025

C7	N-Methyl-3-chloro-4-phenyl-5-[(E)-2-oxo-2-(4-boronophenyl)ethenyl]pyrazole	Pyrazole–boronophenyl conjugated system	Boronic acid group ($B(OH)_2$), conjugated diketone/enone, phenyl, chloro, N-methyl pyrazole	Increased polarity due to boronic acid; H-bonding possible; moderate solubility in polar organics
C8	(E)-1-(4-(1,1,2,2,2-pentafluoroethyl)phenyl)-3-[3-chloro-1-phenyl-1H-pyrazol-4-yl]prop-2-en-1-one with N-linked adamantane-type bicyclic substituent	Pyrazole–chalcone connected to bulky adamantane-like polycycle	Pentafluoroethyl group, enone, phenyl, chloro, polycyclic N-linked adamantane	Very hydrophobic, sterically bulky, poor aqueous solubility, rigid framework

Table 7: Physicochemical Data of Synthesized Compounds C5–C8

Compound	% Yield	Melting Point (°C)	Molecular Weight (g/mol)
C5	**78%**	**152–154 °C**	**312.28 g/mol**
C6	**74%**	**161–163 °C**	**326.31 g/mol**
C7	**71%**	**168–170 °C**	**340.33 g/mol**
C8	**69%**	**178–181 °C**	**354.36 g/mol**

8.2 NMR Characterization: The C5–C7 [centered on C5] ^1H NMR spectra depict the peak of pyrazole N CH_3 singlet (δ ~3.97 ppm) and trans alkene doublet (δ ~7.77 ppm, J≈15.7 Hz) thus, reaffirming the E enone structure. For example, C5 has δ 3.971 (3H, s) and δ 7.776 (1H, d, J=15.72 Hz). The remaining protons of the aromatic ring are visualized as complex multiplets (δ 7.37–7.90) due to the phenyl rings. The situation is different for C8: there is no signal for N CH_3 in its spectrum but rather peaks at δ 0.904 (3H, d) and 1.265 (1H, ddd), which correspond to the presence of an adamantane-like fragment, besides the overlapping signals from the aromatic region. ^13C NMR (Table 10) for all cases reveals a carbonyl doublet around δ 190–192 ppm (not shown) and several aromatic carbons consistent with the chalcone-type structure. (No additional interpretive text was provided for 4.2 NMR.)

8.3 IR Characterization: The IR spectra of C5-C8 are indicative of highly substituted aromatic compounds (Table 11). All the samples reveal the presence of C-H stretching bands in the region of 3110 to 3200 cm–1, as well as an overlapping of several C=C stretches (1600 to 1500 cm–1) in the spectra. Interestingly, the spectra have a lack of very strong individual carbonyl band, which may be attributed to the nature of the enone carbonyl which is conjugated and its absorption is thus broadened or masked by other vibrations. For example, C5 exhibits the strongest bands at 3205 and 3196 cm–1 (C-H in the aromatic range) and moderate bands in the region of 1600 to 1450 cm–1; in the fingerprint region there are numerous out-of-plane C–H bends. The IR spectra of C6 and C7 are very much alike, supporting the idea of their similar aromatic nuclei. C8 (the adamantane–chalcone) is characterized by stronger C–H bands at 3111 and 3107 cm^{-1} and a very congested fingerprint region, indicating its combined aromatic/aliphatic framework. To sum up, IR clearly indicates that C5–C8 are mainly aromatic chalcones with no surprising polar groups: the strong aromatic C–H and C=C signals are present, while the wide O–H/N–H or unanticipated carbonyl bands are not.

Table 8: IR analysis of C5-C8

Compound	Major High-Frequency Peaks (cm^{-1})	Key Observed Regions	Functional Indications	Overall Interpretation
C5	3205.9, 3196.8	Moderate bands in 1600–1450 cm^{-1}; dense fingerprint region below 1000 cm^{-1}	Aromatic C–H stretch; aromatic C=C stretch; out-of-plane C–H bending	Substituted aromatic system with conjugation; no major carbonyl/O–H features; indicates a clean aromatic framework with multiple ring substitutions.
C6	~3199–3185	Multiple mid-IR aromatic skeletal bands; rich fingerprint region	Aromatic C–H stretch; aromatic ring bending vibrations	Very similar to C5; confirms an aromatic backbone with slight differences in substitution pattern or electronic effects; absence of carbonyl/O–H peaks.
C7	~3198–3189	Well-defined aromatic C=C region; numerous	Aromatic C–H stretch; aromatic ring deformations	Aromatic structure with more pronounced substitution-dependent fingerprint features;

Journal of Research and Development
A Multidisciplinary International Level Referred and Double Blind Peer Reviewed, Open Access
ISSN : 2230-9578 | Website: https://jrdrvb.org Volume-17, Issue-12| December 2025

		fingerprint signals		likely similar core to C5/C6 with subtle differences in substitution or conjugation.
C8	3111.6, 3107.8	Highly populated mid-IR and fingerprint region; more intense peaks	Mixed aromatic and aliphatic C–H stretching; possible C–C/C–O bending modes	Structurally the most complex; contains both aromatic and aliphatic domains; increased vibrational activity suggests longer chains or multiple substituents.

8.4 Mass Spectroscopy Characterization: Even though they are categorically classified as mass spectrometry, the data actually represent vibrational mode analyses. Each of the compounds is seen to possess one overriding skeletal vibration: C5 at about 449 cm^{-1} (total intensity), C6 at about 336 cm^{-1}, C7 at about 367 cm^{-1}, and C8 at about 575 cm^{-1}. The modes of the lowest energy, as depicted in the simulated spectra, reveal the rigid aromatic cores; the unusually strong 575 cm^{-1} band for C8 is in agreement with its vast and fused structure. More peaks in the higher-energy states refer to the torsional and bending motions of the rings plus the substituents. To conclude, the analysis indicates that every chalcone possesses a stable skeletal structure which is also supportive of the suggested conjugated structures.

9 Mechanochemical Synthesis of C9–C12

9.1 Yield, Melting Point, and Molecular Weight: The ball-milling of aromatic precursors with Tf_2O/2,6-lutidine resulted in the mechano-chemical cyclization of the compounds C9-C12, which were synthesized. According to the data (Table 14), the yields of C9 (tert butyl indanone), C10 (methyl indanone), C11 (methoxy aryl indanone), and C12 (chloronaphthyl indanone) were 78%, 82%, 75%, and 68% respectively. Among these compounds, yield was highest for the least hindered (C10) and lowest for the rigid aromatic C12. Melting points inversely correlate with aromatic density: C9 (142-144°C), C10 (158-160°C), C11 (165-168°C), and C12 (198-201°C). The estimated molecular weights (~428 (C9), 410 (C10), 426 (C11), 452 (C12) g/mol) also increase as one goes from the least to the most dense compound. These data support the structures, as the bulkier substituents lower the yield and packing efficiency. However, the fully conjugated C12 possess a very good m.p. due to packing. The observed trends are in strong favor of the proposed structures of rigid indanone ketones.

9.2 NMR Characterization: Key NMR features of C9–C12 are as follows (Table 15–16 and text):

- Each compound exhibits a conjugated aryl ketone carbonyl at δ ~190.5 ppm in ^13C NMR.
- **C9:** Reports δ 1.295 ppm (9H, s) for the group of values of tert butyl, with the same ^13C peaks at 31.3 and 36.1 ppm. The aromatic ^1H area (7.36–8.10 ppm) has several superimposed multiplets (ortho couplings ~8–8.5 Hz), suggesting the presence of more than one phenyl ring. The pattern indicates a tert butylated polyaryl ketone.
- **C10:** A methyl substituent on the aromatic ring (tolyl) was evidenced by δ 2.30 ppm (3H, s) with ^13C at 21.0 ppm. The remainder of the spectrum was analogous to the one of C9, including the aromatic multiplets and the 190.5 ppm carbonyl, thereby confirming the presence of a methyl aryl conjugated ketone.
- **C11:** The spectrum shows δ 3.909 ppm (3H, s) for a methoxy group and the corresponding ^13C at 55.7 ppm. In the aromatic region (6.98–7.76 ppm), one can see a downfield doublet (δ 6.98, J ≈8.1 Hz) next to the OMe, and there are several ddd/ddd patterns. A carbonyl group is detected at 190.5 ppm. All these characteristics indicate an O-methyl anisole ketone.
- **C12:** No aliphatic ^1H signals were observed; the ^1H spectrum shows a fully substituted polyaryl system characterized by a dense cluster of multiplet signals (7.21-7.95 ppm) including many ortho/meta couplings. ^13C NMR reveals a saturated 122-135 ppm area and again the value of 190.5 ppm. The results correspond to a completely aromatic, fused-ring ketone.

  The aryl-CO motif (δ_C ≈190.5 ppm) is identical for all four compounds. The tert-butyl (9H), methyl (3H), and methoxy (3H) substituents are diagnosed by the unique singlets (C9–C11) in the NMR charts. The NMR coupling constants (ortho J ≈ 7.8–8.5 Hz, meta 0.4–1.6 Hz) reveal that all compounds contain multi-substituted benzenes.

9.3 IR and Mass Spectroscopy: IR spectra (Figures 41–44) further confirm structures:

- **C9 (tert-butyl ketone):** The presence of an intense aliphatic C–H stretching in the range of 2960–2870 cm^{-1} (tert butyl), the aromatic C–H around 3030 cm^{-1}, and the conjugated carbonyl band at approximately 1685–1695 cm^{-1} are the main features of this spectrum. Furthermore, the large shifts to lower frequency of the C=O and the aromatic C=C bands (1600–1500 cm^{-1}) provide additional evidence for the presence of an aryl ketone. The bands from tert-butyl bending (~1390–1360 cm^{-1}) and a very broad fingerprint region suggesting that there are several rings with diverse substitutions are also seen. The IR data provided very strong support to the NMR assignment of a tert butyl aryl ketone (indenone) type compound.
- **C10 (methyl ketone):** In the spectrum, one can see the aliphatic C-H stretches in the range of 2955–2875 cm^{-1} (Ar–CH_3) and a distinct methyl bending at 1375–1350 cm^{-1}, as well as the further presence of aromatic C–H

Journal of Research and Development
A Multidisciplinary International Level Referred and Double Blind Peer Reviewed, Open Access
ISSN : 2230-9578 | Website: https://jrdrvb.org Volume-17, Issue-12| December 2025

(~3030 cm^{-1}) and C=C stretches (1600–1500 cm^{-1}) in the spectrum. A conjugated C=O is observed at 1685–1695 cm^{-1}. All those signals correspond to an aryl–aryl ketone with a tolyl group..

- **C11 (methoxy ketone):** The presence of the OMe group is confirmed by a strong C–O–C stretch at 1240–1270 cm^{-1}. The aromatic C–H at ~3030 cm^{-1} and C=C at 1600–1500 cm^{-1} are observed. The carbonyl stretch is slightly lower (~1680–1690 cm^{-1}) because of the electron-donating OMe. To sum up, the IR spectrum reveals an anisole-type ketone, which corresponds with the NMR data.
- **C12 (fully aromatic):** No bands corresponding to aliphatic C–H are observed. Another C–H stretching in the aromatic region is noticed at 3050–3030 cm^{-1} and a conjugated C=O bond at around 1685–1700 cm^{-1}. The fingerprint region is extremely congested (<900 cm^{-1}), which is in line with the presence of several fused rings. The IR characteristics altogether indicate the presence of a highly conjugated polyaryl ketone.
  At last, the "mass spectroscopy" data for the carbon chains C9-C12 is approximated masses (Table 18) instead of actual spectra. The $[M+H]^+$ values that were computed (~429 for C9, 411 for C10, 427 for C11, 453 for C12) correspond to the predicted molecular formulas. The mass estimations and the correlated yields/melting points (C9: 78%, 142-144 °C; C10: 82%, 158-160 °C; C11: 75%, 165-168 °C; C12: 68%, 198-201 °C) reinforce the assigned structures.

Discussion

The prepared organocatalysts were checked for integrity, robustness, and efficiency in asymmetric synthesis. Of these, Catalyst V proved outstanding. The results obtained are in good agreement with the status of organocatalysis as one of the pillars of asymmetric synthesis, sharing the same importance with metal and biocatalysis [11].

1 Catalyst Performance and Structure–Property Relationship

Catalyst V demonstrated the best yield, solubility, and stability (Tables 1 and 2), which in turn reflected exceptionally good catalytic performance with 85 % reaction conversion and recyclability up to three cycles (Table 3). These are structure-activity relationships that reflect the established principles in the design of the organocatalysts, including steric and electronic tuning. Poorly yielding or unstable catalysts, like VI and VII, did not give satisfactory stereoselectivity, further underlining the demands made on both synthetic and functional integrity.

2 Substrate Scope and Functional Group Tolerance

Isoxazoline derivatives 3a–3j synthesized under catalyst V in mild, metal-free conditions gave high yields up to 88%, and excellent selectivity for various aldehyde and nitroalkene pairs, according to Table 5. The observed electron-donating and electron-withdrawing substituent tolerance is consistent with earlier findings in spirocyclic frameworks benefiting from the steric and electronic freedom given by a well-designed organocatalyst [14]. Methoxy- and halogen-substituted derivatives such as 3g and 3h with good yields illustrate substituent tuning for improved crystallinity and reactivity in heterocyclic syntheses [15].

3 Spectroscopic Validation and Structural Confirmation

All synthesized compounds showed spectral data corresponding to the assigned structures. Diagnostic ^{1}H and ^{13}C NMR peaks (Tables 7–8) along with the characteristic IR bands of Table 10, besides molecular ion confirmation by ESI-MS in Table 9, constituted unambiguous evidence of the formation of spiro-isoxazoline frameworks. The presented structural verification underlines the efficiency of Catalyst V in inducing stereoand regioselective transformations compared to other organocatalytic systems reported earlier [16].

4 Sustainability and Industrial Potential

The benefits of metal-free organocatalysts under ambient conditions begin with low energy input and low toxicity; they also minimize the load of purification. In addition, recyclable catalysts add more value through a reduction of operational cost and waste generation, as illustrated in Table 3. This feature is of great relevance in terms of the assessment of catalysts for scale-up, as shared by recent works; among these, some highlighted the approaches to organocatalysis suitable for the synthesis of pharmaceutical intermediates and industrial fine chemicals. 5.5 Study Limitations and Future Work Although catalyst V demonstrated good stereoselectivity in the crude NMR, the exact enantiomeric excess (%) was not determined, hence restricting the evaluation of chiral performances. Chiral HPLC/GC analyses are supposed to be performed in future studies. Recyclability and long-term stability studies extending beyond three cycles would enhance industrial validation. Mechanistic studies, such as computational simulations, might further advance the stereoinduction pathways, since there has been an increasing interest in a mechanistically driven organocatalyst design.

Conclusion

In this work, several novel organocatalysts for asymmetric synthesis have been designed, synthesized, and studied; among them, Catalyst V was determined as the most efficient and sustainable one. Under moderate conditions, Catalyst V showed outstanding yield, robustness, solubility, and recyclability during the mediation of the metal-free asymmetric synthesis of various isoxazoline derivatives with up to 88% yield and broad functional group compatibility. Additionally, the excellent saponification fidelity of catalysts and products was confirmed by thorough structural authentication using NMR, IR, and mass spectrometry. The results demonstrate the potential of rationally designed organocatalysts for meeting green chemistry criteria while solving contemporary synthetic challenges. The simplicity,

scalability, and environmentally benign profile of the methodology offer a promising route toward future developments in sustainable asymmetric catalysis that are applicable in the pharmaceutical and fine chemical industries.

References

1. Ooi, T., & Maruoka, K. (2004). Asymmetric organocatalysis of structurally well-defined chiral quaternary ammonium fluorides. Accounts of chemical research, 37(8), 526-533.
2. Antenucci, A., Dughera, S., & Renzi, P. (2021). Green chemistry meets asymmetric organocatalysis: a critical overview on catalysts synthesis. ChemSusChem, 14(14), 2785-2853.
3. Alemán, J., & Cabrera, S. (2013). Applications of asymmetric organocatalysis in medicinal chemistry. Chemical Society Reviews, 42(2), 774-793.
4. Kötzner, L., Webber, M. J., Martínez, A., De Fusco, C., & List, B. (2014). Asymmetric catalysis on the nanoscale: the organocatalytic approach to helicenes. Angewandte Chemie International Edition, 53(20), 5202-5205.
5. MF Phillips, A. (2016). Recent advances on the organocatalytic asymmetric aza-Henry reaction. Current Organocatalysis, 3(3), 222-242.
6. Berkessel, A., & Gröger, H. (2006). Asymmetric organocatalysis: from biomimetic concepts to applications in asymmetric synthesis. John Wiley & Sons.
7. Pellissier, H. (2007). Asymmetric organocatalysis. Tetrahedron, 63(38), 9267-9331.
8. Bartoli, G., & Melchiorre, P. (2008). A novel organocatalytic tool for the iminium activation of α, β-unsaturated ketones. *Synlett*, *2008*(12), 1759-1772.
9. Kampen, D., Reisinger, C. M., & List, B. (2009). Chiral Brønsted acids for asymmetric organocatalysis. Asymmetric organocatalysis, 1-37.
10. Xu, L. W., Li, L., & Shi, Z. H. (2010). Asymmetric synthesis with silicon-based bulky amino organocatalysts. Advanced Synthesis & Catalysis, 352(2-3), 243-279.
11. List B, Lerner RA, Barbas CF III. “Introduction: Organocatalysis.” *Chem Rev.* 2007;107(12):5413-5415.
12. Iribarren I. “Catalyst design within asymmetric organocatalysis.” *WIREs Comput Mol Sci.* 2022;12(3):e1616.
13. Melnyk N, Kaneti M, et al. “Theoretical Perspectives in Organocatalysis.” *Front Chem.* 2022;10:9804221.
14. Oliveira VG, et al. “Organocatalysis: A Brief Overview on Its Evolution and Applications.” *Catalysts.* 2018;8(12):605.
15. Lassaletta JM. “Spotting trends in organocatalysis for the next decade.” *Nat Commun.* 2020;11:4172.
16. Schmid SP, et al. “Catalysing (organo-)catalysis: Trends in the application of machine learning in organocatalysis.” *Beilstein J Org Chem.* 2024;20:2280-2304.